Optically-isotropic nanoencapsulated liquid crystal displays based on Kerr effect

Seung-Gon Kang[1,2] and Jae-Hoon Kim[1,*]

[1]Department of Electronic Engineering, Hanyang University, Seoul, 133-791, South Korea
[2]Image Lab Corp., Room 201, AITA, Wongok-Dong, Danwon-Gu, Ansan-Si, Gyeonggi-Do, 425-849, South Korea
*jhoon@hanyang.ac.kr

Abstract: An innovative liquid crystal display (LCD), incorporating in-plane switching mechanism with LC nanoencapsulation, is developed and its electro-optic (EO) performances are characterized. The nanoencapsulated LCDs exhibit electric-field induced transitions from an optically-isotropic state to an anisotropic one based on Kerr effect. Extremely small size of LC droplets embedded in the nanoencapsulated layer, less than a quarter of wavelength of incident light, appear transparent in the voltage-off state and gradually becomes birefringent in response to applied voltage, exhibiting the optical behavior of uniaxial retarder. Due to optically-isotropic nature and a large Kerr effect, they show wide viewing angle characteristics and good EO performances.

OCIS codes: (230.3720) Liquid-crystal devices; (220.4241) Nanostructure fabrication.

References and links

1. J. L. Fergason, "Polymer encapsulated nematic liquid crystals for displays and light control approaches," SID Symp. Dig. **16**, 68 (1985).
2. Q. Wang, J. O. Park, M. Srinivasarao, L. Qiu, and S. Kumar, "Control of polymer structures in phase-separated liquid crystal-polymer composite systems," Jpn. J. Appl. Phys. **44**(5A), 3115–3120 (2005).
3. S. J. Jang, J. W. Jung, H. R. Kim, M. Y. Jin, and J. H. Kim, "Stability-enhanced pixel-isolated method for flexible liquid crystal displays," Jpn. J. Appl. Phys. **44**(9A), 6670–6673 (2005).
4. M. J. Sansone, G. Khanarian, and M. S. Kwiatek, "Large Kerr effects in transparent encapsulated liquid crystals. II. Frequency response," J. Appl. Phys. **75**(3), 1715 (1994).
5. E. A. B. Saleh and M. C. Teich, *Fundamentals of Photonics* (John Wiley & Sons, 1991) p. 696.
6. J. H. Kim, S. D. Lee, and S. Kumar, "Alignment of liquid crystals on polyimide films exposed to ultraviolet light," Phys. Rev. E Stat. Phys. Plasmas Fluids Relat. Interdiscip. Topics **57**(5), 5644–5650 (1998).
7. T. Kissel, S. Maretschek, C. Packhauser, J. Schneiders, and N. Seidel, in *Microencapsulation*, ed. S. Benita (CRC Press, New York, 2006), p. 103.
8. K. S. Bae, Y. J. Lee, C. J. Yu, H. J. Lee, J. H. Park, and J. H. Kim, "Low voltage and High Transmittance Polymer-Stabilized Blue-Phase Liquid Crystal Device by Combined In-Plane and Oblique Electric Field along the Horizontal Direction," Jpn. J. Appl. Phys. **51**, 072201 (2012).
9. S. Yoon, M. Y. Kim, M. S. Kim, B. G. Kang, M. K. Kim, S. W. Kang, S. H. Lee, W. S. Kang, and G. D. Lee, "Analysis of electro-optic characteristics of polymer-stabilized blue phase liquid crystal driven by in-plane and fringe electric field," Mol. Cryst. Liq. Cryst. (Phila. Pa.) **529**(1), 95–101 (2010).
10. Z. Ge, L. Rao, S. Gauza, and S. T. Wu, "Modeling of blue phase liquid crystal displays," J. Disp. Tech. **5**(7), 250–256 (2009).
11. Z. Ge, S. T. Wu, S. S. Kim, J. W. Park, and S. H. Lee, "Thin cell fringe-field-switching liquid crystal display with a chiral dopant," Appl. Phys. Lett. **92**(18), 181109 (2008).
12. Y. Haseba, H. Kikuchi, T. Nagamura, and T. Kajiyama, "Large electro-optic Kerr effect in nanostructured chiral liquid-crystal composites over a wide-temperature range," Adv. Mater. **17**(19), 2311–2315 (2005).
13. J. Yan, H. C. Cheng, S. Gauza, Y. Li, M. Jiao, L. Rao, and S. T. Wu, "Extended Kerr effect of polymer-stabilized blue-phase liquid crystals," Appl. Phys. Lett. **96**(7), 071105 (2010).
14. H. S. Choi, G. Higuchi, and H. Kikuchi, "Fast electro-optic switching in liquid crystal blue phase II," Appl. Phys. Lett. **98**(13), 131905 (2011).
15. J. H. Jung, K. S. Ha, M. N. Chae, W. S. Kang, G. D. Lee, and S. H. Lee, "Abnormal behavior in colour tracking characteristics of the fringe-field switching liquid crystal display," Liq. Cryst. **37**(3), 303–309 (2010).
16. J. Yan, L. Rao, M. Jiao, Y. Li, H. C. Cheng, and S. T. Wu, "Polymer-stabilized optically-isotropic liquid crystals for next-generation display and photonics applications," J. Mater. Chem. **21**(22), 7870 (2011).

1. Introduction

Nowadays liquid crystal display (LCD) technology can be generally acknowledged to reach maturity since its major obstacles are mostly eliminated. The viewing angle issue has been almost solved by using multi-domain device structure and optical compensation films. The response time issue has also been improved to a few milliseconds by employing an overdrive method as well as a sophisticated control technique of LC pretilt angle via a precise manipulation of reactive mesogens. And the low contrast ratio issue has been nearly alleviated due to the advent of novel local dimming technique of the light emitting diode (LED) backlight, currently exceeding over 10,000:1. However, in the flat panel display (FPD) arena, with excellent products and fierce competition, in order for the LCD industry to get more solid competitive edge over other competitors, there are still other remaining issues to be overcome such as how to reduce the production cost substantially and how to make it flexible. A variety of innovative activities are known to be done to cut down the cost of LCDs such as elimination or reduction of core materials and renovation of manufacturing processes. And much more active research has been done on the development of flexible LCDs through various approaches like polymer dispersed liquid crystal (PDLC) [1], polymer-network liquid crystal (PNLC) [2], and pixel-isolated liquid crystal (PILC) [3], etc. However, so far any up-to-date technologies have never suggested simultaneous solution of these imminent problems: low cost and flexibility.

In this paper, we report the development of an entirely new display mode, nanoencapsulated liquid crystal display, which is believed to have the potential to resolve the remaining urgent issues in LCD industry. This emerging LCD technology which combines state of the art LC nanoencapsulation with in-plane switching mechanism exhibits the following distinct features. (1) Its cell fabrication process is quite simple and cost-effective because it does not require any alignment layers and is free of assembly due to adoption of a single-substrate structure. (2) The voltage-off state is optically isotropic due to extremely small particle size effect of LC nanocapsules embedded in the nanoencapsulated layer and voltage-on state forms multi-domain structures to be determined by the configuration of in-plane electrodes, so that the viewing angle is wide and symmetric. (3) It shows good compatibility with flexible display because it just can be manufactured with a printing method taking advantage of both LC nanocapsules and a single-substrate structure, instead of a conventional LC injection one which indispensably requires an assembly process between upper and lower substrates. We report the fundamental switching principles of this novel LCD technology including electro-optic performances by analyzing Kerr effect and overall fabrication processes. Additionally, viewing angle characteristics of the nanoencapsulated LCD will be characterized.

2. Operating principle

As shown in Fig. 1, the principal feature of our novel LCD consists in the unique constructions which are composed of a nanoencapsulated LC layer and a single substrate equipped with in-plane switching (IPS) electrodes. The nanoencapsuated LC layer is consisted of LC embedded in a polymeric binder matrix in the form of nanocapsules. In general, when the droplet size of LC in a medium is approximately equal to the wavelength of incident light, the medium is highly scattering and consequently translucent to quite opaque [4]. When the size of LC droplets is much smaller than the wavelength of the incident light, the incident light became transparent than opaque through the medium since the light scattering is substantially attenuated. In our proposed LCD, the size of nanocapsules embedded in the nanoencapuated LC layer is less than 150 nm which is about a quarter smaller than the wavelength of the visible light, the nanoencapsulated LC layer is optically transparent at the initial state (i.e. voltage-off state). In the strict sense, its optically isotropic nature arises from dual effects of both extremely small size of LC nanocapsules and a random distribution of LC molecules inside of them at the voltage-off state. Because the LC

molecules are arbitrary arranged in the nanocapsules, the nanoencapsulated LC layer shows the optically isotropic characteristics at the voltage-off state.

An upper enlarged diagram in Fig. 1(a) shows how the nanoencapsulated LCDs operate upon the application of a bias voltage. The LC molecules confined inside the individual nanocapsules are randomly distributed at the voltage off state and tend to reorient along the direction of the electric field at voltage-on state, which induce the retardation. Unlike the case of voltage off-state, optically isotropic, the nanoencapsulated LC layer becomes optically anisotropic due to the collective reorientation of LC molecules along the same horizontal direction of electric field caused by IPS electrode architecture, thereby leading to the generation of induced birefringence. Such a phenomenon as the electric field-induced birefringence is identical to that of Kerr effect [5].
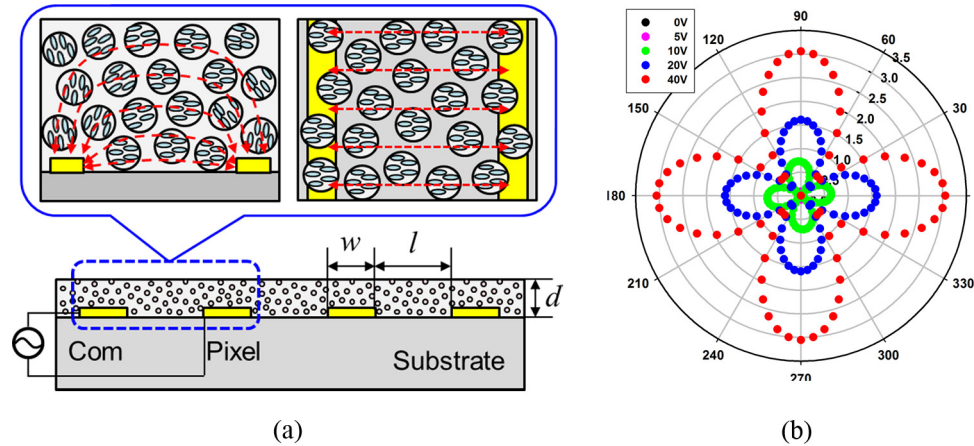

Fig. 1. (a) A schematic diagram depicting a device configuration of the nanoencapsulated LCD and how it operates, where the upper two magnified ones indicate the cross-sectional and horizontal view showing how LC molecules inside each nanocapsule are oriented upon the application of a bias voltage, respectively. (b) Measured angular optical anisotropy of the nanoencapsulated LCD with respect to varying applied voltages.

The unusual phenomenon of induced birefringence based on Kerr effect could be also verified with the measurement on the angular optical anisotropy of the nanoencapsulated LCD with respect to increasing applied voltages, as shown in Fig. 1(b). With the conventional birefringence measurement setup consisting of photoelastic modulator (PEM90, Hinds Instruments), He-Ne laser, and two crossed polarizers, the angular phase retardation of the nanoencapsulated LCD was measured while rotating the sample with respect to the surface normal to the incident laser beam for a certain bias voltage [6]. As can be seen from the polar diagram with respect to the applied voltage, no optical anisotropy is detected at the voltage-off state (0V) due to the unique nature of the nanoencapsulated LCD, whereas phase retardation increases proportionately to a bias voltage applied on it. Since the optic axis of the nanoencapsulated LCD induced by the applied electric field is perpendicular to the direction of striped electrodes of IPS panel, as shown in the upper right diagram of Fig. 1(a), which in turn looks like a uniaxially varying retarder plate, its polar diagram of phase retardation shows up a 4-fold symmetry, 90° of angular periodicity.

3. Experiments

3.1 Preparation of LC nanocapsules

We adopted a conventional coacervation [7] as a fabrication method of LC nanoencapsulation in this development. Since the representative physic-chemical method is usually used for microencapsulation, state of the art technology of LC nanoencapsulation needs to be developed, whose detailed fabrication process are followed. At first, a nematic host LC is

added to mixture of nonionic polymeric surfactants and emulsifier dissolved in aqueous solution, where the polymeric surfactant and emulsifier play an important role of reducing surface tension and forming a shell material of LC droplet, respectively. According to our experiment, the smallest mean diameter of LC droplets which can be achieved without use of the polymeric surfactant seemed to be ~300nm. It seems to be practically unavailable to reduce the size of LC droplets less than 300nm without using the polymeric surfactant, signifying the crucial role of the surfactant in LC nanoencapsulation process. As a polymeric surfactant we selected one of copolymers which are well matched with a nematic host LC, polyethylene oxide-polypropylene oxide-polyethylene oxide (PEO-PPO-PEO) block copolymers (Pluronics®, BASF). And PVA (polyvinyl alcohol, partially-hydrolyzed, 88%, Aldrich), a water-soluble polymer, is adopted as a shell-forming material as well as an emulsifier due to its good optical transparency and chemical inertness with LCs. Then the immiscible mixture is homogenized using a high-pressure homogenizer with a pressure range generally between 10,000 and 20,000 psi in a room temperature, resulting in the formation of oil in water (O/W) nanoemulsions. This initial emulsification process is greatly important since it will usually determine the overall size distribution of LC nanocapsules. Next, these O/W nanoemulsions are heated up to a cloud point, about 50 °C, the critical temperature above which an aqueous solution of water-soluble emulsifier, PVA, becomes turbid, and are kept at that temperature for several hours while being stirred so as for PVA to be phase-separated around the nano-sized LC droplets, thereby forming a thin polymeric shell surrounding each of them. Finally, such nano-sized LC droplets encircled with such a thin polymeric membrane in the nanoemulsions are chemically crosslinked by the addition of crosslinking agents such dialdehydes as glutaraldehyde, formaldehyde, and glyoxal, etc., which leads to reinforcing each of them with good flexibility and durability. This final crosslinking process is indispensable to get the LC nanocapsules durable enough to endure a certain degree of external forces. Otherwise, the LC nanocapsules are so immature that they can get easily damaged or disrupted in the post manipulation process of themselves.
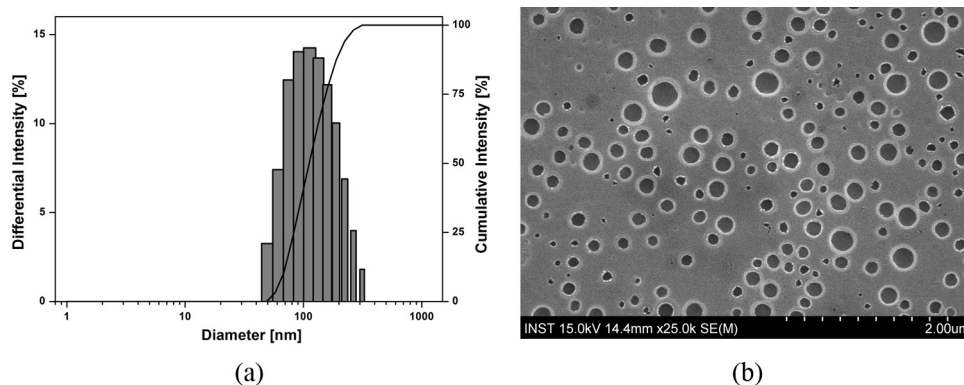

Fig. 2. (a) Particle size distribution data of the LC nanocapsules prepared by a coacervation method and (b) SEM images taken after the LC nanocapsules are coated on the substrate.

Figure 2(a) shows the typical particle size distribution data of our LC nanocapsules obtained by the above-mentioned coacervation method. The mean diameter was measured to be about 110nm which is one fourth smaller than the wavelength of incident light (λ = 550nm), and its polydispersity index was 0.095, measured by the apparatus of ELSZ (Otsuka Electronics Co., Japan). As can be seen from the Fig. 2(a), the measurement data assure that the LC nanocapsules conform to a normal distribution as identical as that of a standard particle. As another convincing way to check the size distribution of LC nanocapsules, optical inspection is also performed to get SEM images, as shown in Fig. 2(b), which is taken after the LC nanocapsules are coated on the substrate. It clearly shows that LC nanocapsules, which are shown as tiny circular holes, are randomly dispersed in the polymeric binding matrix. From metrology on the diameter of holes appeared in Fig. 2(b), the largest one among

them is estimated to be less than about 200 nm, verifying that size distribution data of the LC nanocapsules in Fig. 2(a) are consistent with those of optical method.

3.2 Fabrication of nanoencapsulated LC layer and LC Cell

After completion of preparing the LC nanocapsules as mentioned above, the LC nanocapsules need to be converted to a coating solution in order for them to be coated on the substrate, since they can't be printed directly on the substrate by themselves due to high level of surface tension. In order to using the printing method for LC layer, the LC nanocapsules should be mixed with a suitable amount of binders and plasticizers, which would adjust their surface tension to maintain appropriate printability.

First of all, the LC nanocapsules should be separated from an aqueous solution consisting of LC nanocapsules, some remaining emulsifiers, and mostly water solvent using an ultracentrifugation, a process which nano-sized particles dispersed in the continuous phase are usually centrifuged to sedimentation since their particle size is too small in contrast to micro-sized ones. Then the separated LC nanocapsules are mixed with an appropriate amount of binder and plasticizer, where hydrophilic PVA (Fully-hydrolyzed, 99%, Aldrich) and ethylene glycol are employed as a binder and plasticizer, respectively. The reason why we chose PVA as a binder, the same substance as a shell-forming polymer, is to get better optical transmittance in the visible spectrum range through a perfect synchronization with the index of refraction. The only distinction in material property between a shell-forming PVA and a matrix-forming one is the degree of hydrolysis which determines physical characteristics such as membrane strength and rigidness. The higher the degree of hydrolysis makes the stronger membranes. Mixture ratio between each compound directly affects the rheological properties of the nanoencapsulated LC coating solution. Thus we optimized the mixing ratio in the coating solution from the viewpoint of uniformity in the coated layer and how much density of LC nanocapsules in the nanoencapsulated LC layer is the most appropriate for producing better electro-optical performances.

The coating solution prepared with an optimized mixing ratio between LC nanocapsules, binder, and plasticizer is printed directly onto a device substrate whose electrodes are patterned into IPS architecture. Since the IPS electrode structure only needs the patterned electrode on one substrate, there is no necessary of the upper substrate and the precise assembly process even if we use two substrates. Among a variety of coating methods such as an applicator, an edge coater, a screen printer, a bar coater, and a slot-die coater, we adopted a bar coater because it is quite simple and convenient to control the process conditions. Next, a drying step is conducted in which the solvent is evaporated from the coated LC nanoencapsulation layer formed on the device substrate by the coater. According to the unique characteristic of LC nanocapsules which are soft, flexible, and deformable by external forces, the individual LC nanocapsules dispersed in the coated LC nanoencapsulation layer tend to be deformed easily in a shape due to intense liquid flow at dried end portions when their dry rate is too fast. Therefore the solvent drying rate needs to be controlled adequately. From an optimization experiment, we found the optimum drying rate of solvent water to be around 50 °C for more than 2 hours in the oven. As the solvent evaporates, the thickness of the coated LC nanoencapsulation layer decreases, which in turn causes the individual LC nanocapsules to be gradually moved and packed more and more densely. When the solvent has completely evaporated, a LC nanoencapsulated display layer can be obtained with a maximized packing density of the LC nanocapsules embedded in the polymeric binder, which has a flat surface with negligible irregularities due to the advantage of smaller size effect in nanometers.

4. Results and discussion

4.1 Electro-optic performances

Since the nanoencapsulated LCDs operated by an IPS architecture work like a uniaxial retarder plate whose retardation value is varied by the electric field strength of applied

voltage, their transmittance characteristics between two crossed polarizers can be expressed as [8, 9]

$$T(V,\lambda) = T_0 \sin^2 2\Psi(V) \cdot \sin^2(\pi d\Delta n_i(V)/\lambda) \qquad (1)$$

where Ψ is the voltage-dependent angle between the optic axis of LC molecules within nanocapsules and the transmission axis of the polarizers (Ψ is 45° in this work), Δn_i is the voltage-dependent induced birefringence, d is the thickness of the coated LC nanoencapsulated layer, and λ is the wavelength of the incident light. Before applying a bias voltage, the nanoencapsulated LCDs appear dark because there is no birefringence due to optically-isotropic nature in voltage-off state. With a bias voltage, the induced optical birefringence (Δn_i) gradually increases from zero and saturates to the maximum induced birefringence (Δn_0) as applied electric field (E) exceeds the saturation electric field (E_s) which is well expressed in the extended Kerr effect as shown in Eq. (2) [10]; hence the transmittance starts to occur.

$$\Delta n_i = \Delta n_0[1 - \exp(-(E/E_s)^2)] \qquad (2)$$

We prepared a test panel device with IPS electrodes on the glass substrate, which has 3um pattern width (w) and 6um pattern spacing (l) for pixel and common electrodes, respectively. Then the LC nanocapsules manufactured following the processes as mentioned above, the mean diameter of about 110nm, are converted into a coating solution and its coating solution is just coated on the test panel using a bar coater, which finally leads to a nanoencapsulated LC layer on the substrate, the resultant dried thickness (d) of about 4.6um. We used a nematic host LC material with high birefringence ($\Delta n \sim 0.23$) and large dielectric anisotropy ($\Delta \varepsilon \sim 40$) in order to get as large Kerr effect as possible. The LC nanoencapsulated test panel was sandwiched between two crossed polarizers with the striped electrodes oriented at 45° with respect to the transmission axis of polarizers. As shown in Fig. 3, three insets are the microscopic images of the nanoencapsulated LC device taken at three different bias voltages (0V, 15V, and 30V), where the narrow dark and wide bright lines correspond to patterned electrodes ($w = 3.0$um) of light-blocked region and electrode pattern spacing ($l = 6.0$um) of light-transmitted one, respectively. The image shows clearly that the transmittance of nanoencapsulated LC devices is fully saturated even in the low driving voltage of 30 V.
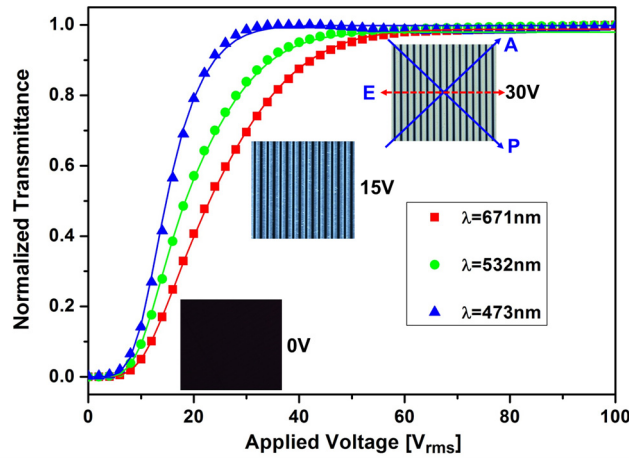

Fig. 3. Normalized voltage-transmittance characteristics of the nanoencapsulated LCDs at three different wavelengths which correspond to blue (473nm), green (532nm), and red (671nm), respectively. Measured and fitted data for each wavelength are denoted as filled dots and solid lines. Three insets are POM images taken at different bias voltage, where P, A, E denote the directions for polarizer, analyzer, and electric-field, respectively.

The corresponding voltage-dependent transmittance curves were measured at room temperature (T~23 °C) for three different wavelengths (473 nm, 532 nm, and 671 nm) using laser light sources, as shown in Fig. 3. In a conventional nematic IPS or FFS cell, the on-state LC profile forms the vertical structure of two connected TN cells with reverse twist sense [11], thus there is a self-compensation for wavelength dispersion from this special two-TN-cell profile, resulting in the revelation of very small wavelength dispersion. But in the nanoencapsulated LCDs, since the transmittance arises from pure phase retardation effect, similar to a vertical alignment (VA) cell, the dependence on the wavelength of probing radiation used in this experiment becomes relatively larger compared to that of nematic IPS or FFS cell. However, different from the nematic VA cell, the induced birefringence (voltage-on state) of the nanoencapsulated LCDs has multi-domain structure originating from the electric field profiles as shown in Fig. 1(a), where horizontal fields dominate between electrode gaps and vertical components flourish above the electrode surface [10].

Taking into account the similarity in the operating mechanism with PSBP-LCDs, we simulated the voltage-transmittance characteristics using the extended Kerr effect [12–14]. In Fig. 3, the filled dots represent experimental data and solid lines are simulated results. Because the electric field distribution is non-uniform caused by the electrode configuration of IPS cell, the local induced birefringence was calculated based on the electric field distribution taking into account the saturation phenomenon described by the extended Kerr effect. Then we further assign the local optic axis direction of each unit along the electric field vector. From this consideration, the transmittance in Eq. (1) can be modified as follows [15]:

$$T/T_0 = \sin^2 2\Psi(V) \cdot \sin^2(\alpha \pi d \Delta n_i(V)/\lambda) \qquad (3)$$

where α is a weighting factor, one of three fitting parameters related to the transmittance and effective phase retardations. Other two fitting parameters, Δn_0 and E_s, which are not shown explicitly in Eq. (3) but expressed in Eq. (2), stands for the saturated induced birefringence and the saturation electric field, respectively. Three fitting parameters and their resultant Kerr constant at each wavelength are listed in Table 1.

Table 1. Voltage-transmittance curve fitting results of weighting factor (α), saturated induced birefringence (Δn_0), saturation electric field (E_s), and Kerr constant of the nanoencapsulated LCDs at three wavelengths.

λ (nm)	α	Δn_0	E_s (V/um)	K (nm/V^2)
473	0.54	0.099	2.8	26.7
532	0.63	0.096	2.8	23.0
671	0.76	0.092	2.8	17.5

As shown in Table 1, in spite of using a nematic LC material with high dielectric anisotropy ($\Delta\varepsilon = 40$) and large optical anisotropy ($\Delta n = 0.23$), the nanoencapsulated LCDs produce the extraordinary characteristics of quite large Kerr constant K ~23.0 nm/V^2 (at 532 nm), about 5 to 10 times higher than the conventional PSBP-LCDs [16]. Exhibiting such a unique feature of extremely large Kerr constant in the nanoencapsulated LCDs is attributed to the following reasons. In the case of PSBP-LCDs, LC materials should be doped with a relatively large amount (typically 10~30 wt%) of chiral dopants so as to be changed from nematic to blue phase [16]. Generally, chiral nematic phase LCs doped with some amount of dopants are known to have higher elastic energy than that of normal nematic phase LCs, thereby resulting in an elevated operating voltage. On the contrary, since the only nematic host materials are used in the fabrication of the nanocapsulated LCDs, free of chiral dopants, a higher Kerr constant can be achieved, resulting in low driving voltage. And also, both smaller electrode width ($w = 3.0$ μm) and inter electrode spacing ($l = 6.0$ μm) can contribute to create a larger Kerr effect.

Different from the cases of α, Δn_0 and K, it is quite interesting to note that the fitting parameter E_s remains invariant for all the wavelengths studied. The dispersion-free property

of E_s value with respect to wavelength can be explained as follows: at a given voltage the LC director reorientation profile in the nanoencapsulated LCDs is purely determined by the balance between elastic and electric torques and the LC director distribution will not be affected by the probing wavelength [10]. On the other hand, saturated induced birefringence (Δn_0) and weighting factor (α) are apparently dependent on the wavelength since the phase retardation is an intrinsic term varying with wavelength. The saturated induced birefringence (Δn_0) is 0.096 (at 532nm), about 1/3 of intrinsic birefringence ($\Delta n = 0.23$ at 589 nm) of host nematic LC employed, which is reasonable one from the viewpoint of extended Kerr effect.

4.2 Viewing angle characteristics

Generally a display medium showing optically isotropic property in the voltage-off state is most preferred especially in LC-modulating devices because it is very advantageous for achieving wide viewing angle characteristics. In that sense, the nanoencapsulated LCDs have an outstanding merit that it behaves like an optically isotropic medium in the voltage-off state since it is intrinsically transparent due to its much smaller particle size effect of nanometer embedded in the polymeric binder, as mentioned earlier. As a result, the light leakage in the initial dark state only occurs at an off-axis incidence since two crossed polarizers at a normal incidence is no longer perpendicular to each other at an oblique angle of incidence.

However, in the voltage-on state, since the optic axis of the induced birefringence is determined by the electrode design configuration in an IPS cell, the viewing angle performances are quite dependent on the profile from its electric field distribution. As noted above, in this work, only a single domain profile is produced because the electrode configuration in IPS test panel is designed with 2-domain lengthwise striped patterns, not a zigzag one. Figure 4 shows the measured viewing angle characteristics of the nanoencapsulated LCDs without any compensation film. As can be seen from Fig. 4(c), the viewing angle characteristics are more symmetric even using an IPS electrode structure with only 2-domain lengthwise striped patterns and shows the similar viewing cone comparable to that of a conventional 4-domain IPS structure of zigzag electrodes [15]. In order to increase the viewing angle wider, the nanoencapsulated LCDs need to be compensated with both uniaxial films (A-plate) and biaxial films (C-plate) to suppress the light leakage at dark state and can be further expanded by adopting the 4-domain IPS structure of zigzag electrodes whose chevron angle should be 90° as compared to an obtuse angle (> 90°) in the conventional IPS-LCDs.
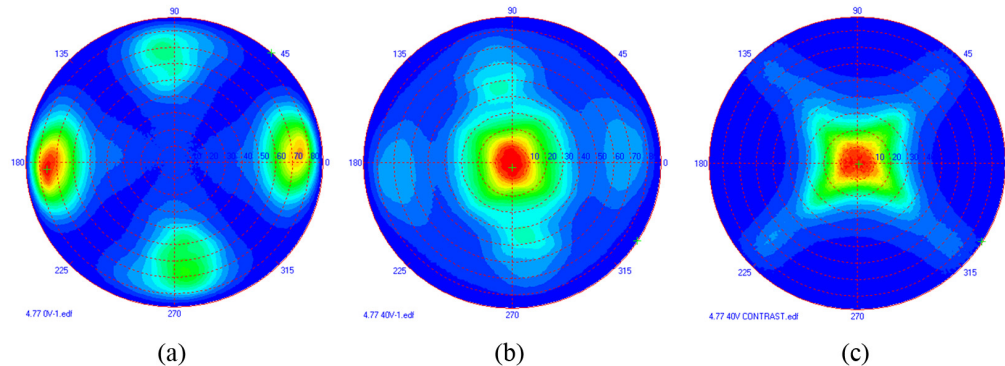

(a)   (b)   (c)

Fig. 4. Measured viewing angle performances of the nanoencapsulated LCDs, where (a), (b), and (c) correspond to off-state luminance (0V), on-state luminance (30V$_{rms}$) and iso-contrast contour, respectively (EZ-Contrast, Eldim).

5. Conclusion

We developed a novel optically transparent nanoencapsulated LCD exhibiting a large Kerr effect. Due to the combination effect of LC nanoencapsulation technology and in-plane

switching mechanism, it shows very unique features as follows: (1) greatly simplified manufacturing process resulting from both no need of alignment layer and a single-substrate fabrication by a printing method, and (2) a good EO performance of wide viewing angle caused by optically-isotropic nature in the voltage-off state. With the nanoencapsulated LCDs fabricated by both LC nanocapsules (mean diameter: ~110nm) and IPS electrode architecture (w = 3.0um, l = 6.0um), we have achieved a low driving voltage of 30 V_{rms} and a contrast ratio of higher than 1,000:1. From the analysis on the measured voltage-transmittance characteristics for three different wavelengths based on the extended Kerr effect, it is confirmed that the nanoencapsulated LCDs exhibit an extraordinarily large Kerr constant of 23.0 nm/V^2 (at 532nm), which is 5 to 10 times higher than that of conventional PSBP-LCDs. So that, the nanoencapsulated LCDs can have potential application for the diverse market of displays due to its superior optical performance as well as its competitive manufacturing cost. In addition, this novel technology, inherently familiar with the flexible display owing to manufacturability by a printing method, can contribute to bring forward the commercialization of the future display device.

Acknowledgments